American Mineralogist, Volume 87, pages 822–828, 2002

H_2O activity in H_2O-N_2 fluids at high pressure and temperature measured by the brucite-periclase equilibrium

ANDREAS HAEFNER,[1,*] LEONID Y. ARANOVICH,[2] JAMES A.D. CONNOLLY,[1] AND PETER ULMER[1]

[1]Institute for Mineralogy and Petrography, ETH-Zentrum, CH-8092 Zurich, Switzerland
[2]Institute of Experimental Mineralogy RAS, Chernogolovka 142432, Russia

ABSTRACT

We present experimental results constraining water activity in H_2O-N_2 fluids containing 40–90 mol% water at pressures of 6–13 kbar and temperatures of 680–840 °C. In the experiments, the displacement of the brucite dehydration equilibrium was used as a gauge of water activity. The experiments were performed in a conventional piston-cylinder apparatus, with NaCl pressure medium and silver azide, AgN_3, as a source of nitrogen. Reversals of the dehydration reaction were used to bracket the equilibrium fluid compositions within 3 mol% H_2O. Water activities were computed from the equilibrium brucite dehydration conditions in pure H_2O as determined by Aranovich and Newton (1996) using thermodynamic data of Holland and Powell (1998). The experimentally derived activities were fit to a van Laar-type equation that reproduces our compositional data with a standard error of 1.6 mol% H_2O:

$$RT \ln\gamma_1 = (X_2)^2 W\{V_1^0 (V_2^0)^2/[(V_1^0 + V_2^0)(X_1V_1^0 + X_2V_2^0)^2]\}$$

where γ_1 is the activity coefficient of H_2O, X_i is the mole fraction of end-member i (1 = H_2O and 2 = N_2), V_i^0 is the molar volume of the pure end-member at the pressure (P) and temperature (T) of interest, and W is analogous to a regular solution parameter. The parameter W was fit as a function of pressure and temperature by the expression $W = (A - BT)[1 - \exp(-20P)] + C \cdot P^{0.3}T$, with A = 40005 J, B = 51.735 J/K, C = 14.848 J/(K·kbar$^{0.3}$), P in kbar and T in K. With these expressions, activity-concentration relations in H_2O-N_2 fluids can be reconstructed in a broad P-T-X range using any equation of state (EOS) for pure H_2O and N_2. The activity-concentration relations are similar to the semi-empirical EOS of Duan et al. (2000) and the theoretical EOS of Churakov and Gottschalk (2002a), although the former somewhat underestimates activities within the experimental pressure range whereas the latter appears to overestimate activities of the components at pressure above 20 kbar.

INTRODUCTION

Nitrogen is a common constituent of natural fluids. Nitrogen-bearing fluid inclusions have been reported in minerals from a variety of geological settings, including eclogite (e.g., Andersen et al. 1989), high-grade metapelite (Janak et al. 1999), magmatic enderbite (Knudsen and Lidwin 1996), ultrahigh-pressure metamorphic rocks (De Corte et al. 1998), and upper mantle ultramafic rocks (e.g., Turner et al. 1990; Andersen et al. 1995; Mohapatra and Murty 2000). In the form of NH_4^+, N can substitute for alkalis in alkali feldspars and micas (e.g., Voncken et al. 1993; Moine et al. 1994). Nitrogen is also found as a major impurity in natural diamonds of kimberlite affinity (e.g., Shiryaev et al. 2000; Boyd et al. 1994), which indicates its potential role in mantle fluids of deep origin. Problems as diverse as metamorphic phase equilibria, interpretation of fluid inclusions and volcanic gas emanations, modeling of planetary atmospheres and interstellar clouds—all require quantitative knowledge of the thermodynamic mixing properties of nitrogen with water at high pressure (P) and temperature (T).

The system H_2O-N_2 has been extensively studied experimentally at temperatures below ca. 400 °C in the pressure range up to 4 kbar (see Anovitz et al. 1998, p. 815–816, for references). Data at higher temperatures and/or pressures are scarce. Chou (1990) measured the water activity (a_{H_2O}) in H_2O-N_2 mixtures over the compositional range $X_{H_2O} = H_2O/(H_2O + N_2)$ = 0.2 – 0.7 at 600 °C and 2 kbar using the H sensor technique, and found a significant positive deviation from the ideal mixing. Anovitz et al. (1998) determined $a_{H_2O} - X_{H_2O}$ relations at 500 °C and 0.5 kbar by the H membrane technique. Their data also indicate large positive deviations from ideality in H_2O-N_2 mixtures. The values for a_{H_2O} derived in the latter study depend strongly upon the thermodynamic data for the Ni-NiO and Co-CoO buffers used to control oxygen fugacity in the experiments (Anovitz et al. 1998).

Supercritical phase separation in the H_2O-N_2 mixtures has been documented recently for the near-critical water isopleths X_{H_2O} = 0.75 (Costantino and Rice 1991) and X_{H_2O} = 0.67 (van Hinsberg et al. 1993) by direct observations in diamond anvil cells in the temperature range 400–560 °C at pressure up to 22

* E-mail: haefner@erdw.ethz.ch

0003-004X/02/0007–822$05.00

kbar. These data are important for constraining the shape of the H_2O-N_2 solvus, but are difficult to use to quantify a_i-X_i relations, due to the large uncertainties in pressure calibration (up to ±2 kbar at temperature above ca. 430 °C; Costantino and Rice 1991, p. 9036) and lack of information on the composition of the N-rich fluid.

This paper presents results of the a_{H_2O} measurements in H_2O-N_2 fluids obtained over a broad pressure, temperature, and compositional range using the brucite (Br) + periclase (Per) + water activity gauge (Franz 1982; Shmulovich et al. 1982; Aranovich and Newton 1996, 1997). An empirical equation describing the mixing properties on the binary join has been calibrated against the experimental data and is compared with the predictions from recent equations of state (Duan et al. 1996, 2000; Churakov and Gottschalk 2002b).

EXPERIMENTAL METHODS

Application of the brucite (Br) – periclase (Per) reaction:

$$Mg(OH)_2 = MgO + H_2O \quad (1)$$

to monitor the H_2O activity in experiments is based on the large buffering capacity of this assemblage due to the high water content of brucite. At any experimental P and T the equilibrium water activity, a_{H_2O}, is calculated from the expression for the total Gibbs free energy of Reaction 1:

$$\Delta G^0_{1,T}(1) + \int_1^P (\Delta V_s)_T dP + RT \ln f^0_{H_2O} + RT \ln a_{H_2O} = 0, \quad (2)$$

where $\Delta G^0_{1,T}$ (1) is the standard Gibbs free energy of reaction 1 at 1 bar and T, $(\Delta Vs)_T$ is the volume change of the solids at T, and $f^0_{H_2O}(P,T)$ is the fugacity of pure water at P and T. Activity-composition relations for H_2O in the H_2O-N_2 fluid are retrieved in conjunction with Equation 2 by using the final fluid composition determined for experiments in which brucite, periclase, and an H_2O-N_2 fluid are presumed to have equilibrated.

Starting materials

The experimental procedure of this study is similar to that of Aranovich and Newton (1996, 1997). A mechanical mixture of synthetic periclase and brucite was used as the starting material. The periclase was originally large limpid crystals of ultrahigh-purity MgO prepared by an arc-fusion method, commercially available from Alfa Aesar (article no. 41648). The brucite was prepared from this periclase by reaction with deionized H_2O at 600 °C and 2 kbar for four days in sealed Au capsules. The result was a 100% yield of pure, coarse-crystalline brucite as determined by both electron microprobe and X-ray diffraction (XRD) analysis. A lightly ground powder mix of the two crystalline substances was prepared in the approximate proportion Br:Per = 1:2, such that the largest XRD peaks were of about the same height. Numerous powder XRD scans of the standard mix in the range 2–70° 2Θ (Cu$K\alpha$) were made to verify reproducibility of the standard pattern. One criterion of the reaction direction of an experiment was change of peak-height ratios of product as compared with those of reactant.

Two compounds have been suggested as a convenient source of N_2 for phase-equilibrium experiments at high pressure and temperature: silver azide, AgN_3 (Keppler 1989), and copper nitride, Cu_3N (Anovitz et al. 1998). Our reconnaissance piston-cylinder runs with Cu_3N + H_2O at 800 °C and 10 kbar showed, however, that the Cu produced on thermal decomposition of Cu_3N was to a large extent converted to Cu_2O due to reaction with H_2O, apparently at the early stages of the experimental run up (because the intrinsic oxygen fugacity of piston-cylinder apparatus is lower than that of the Cu-Cu_2O equilibrium; e.g., Rosenbaum and Slagel 1995). Employing a double-capsule technique with the Ni-NiO-H_2O external oxygen buffer prevented the formation of Cu_2O, but the experiments still failed to produce a consistent N_2 yield. Due to these difficulties with Cu_3N, we resorted to AgN_3 as the N_2 sources in the experiments. This material was prepared and handled as described by Keppler (1989). To test the applicability of AgN_3 for the piston-cylinder experiments, we made "dummy" runs, containing only pre-weighed amounts of AgN_3 and H_2O (Table 1). Analysis of these runs revealed no oxidation of Ag, and showed excellent agreement between the starting amounts of N_2 (in the form of AgN_3) and H_2O weighed in the capsules and those recovered after the runs by a weight-loss method (see below). Another advantage of using AgN_3 is that its N_2 yield is much higher than that of Cu_3N.

The starting materials were loaded into 1 cm long, 0.23 cm OD Pt capsules in the following sequence. First, an aliquot of AgN_3 water suspension was loaded and the capsule was placed in a 1 atm oven at 105 °C for about 10 minutes to dry. After the capsule had reached a constant weight, providing the exact amount of AgN_3 and thus of N_2, the solid Br + Per mix was weighed in, along with a calculated amount of deionized water to give the desired initial fluid composition. The capsule was then sealed by arc welding and re-weighed to ensure that no significant weight loss occurred due to welding. A typical charge consisted of about 4–5 mg of powder mix, 2–3 mg of AgN_3 and 0.3–2 mg H_2O. The amount of powder mix was sufficient to absorb or release about 0.5–0.7 mg of H_2O by the brucite-periclase reaction 1.

Apparatus and run procedure

A 22-mm-diameter, non-end-loaded piston-cylinder apparatus (Johannes 1973) with NaCl pressure medium and graphite heater sleeve was used in this study. In most runs, two capsules were placed horizontally side-by-side in the apparatus and run simultaneously. It was usually possible to choose the composition of the initial fluid phase of the two capsules so that a tight bracket of the final fluid phase was obtained in a single experiment.

A calibrated W–3% Re vs. W–25% Re thermocouple was in virtual contact with the Pt capsules in the experiments, and the run temperature was controlled using an "Eurotherm 902" controller monitored by computer. Temperature fluctuations during the runs did not exceed 1 °C. No correction was made for the effect of pressure on the thermocouple emf. Overall temperature uncertainty of the experiments is estimated as ±5 °C.

The experiments were brought to a pressure about 3–4 kbar lower than the final run pressure at room temperature, then

TABLE 1. Experimental results on decomposition of silver azide at 13.3 kbar

Run no.	T(°C)	Starting materials, mg:			Run products, mg:		X_{H_2O}	
		AgN_3	N_2 nom	H_2O	N_2	H_2O	nom.	measured
AGN1	780	2.33	0.65	0.00	0.67	0.00	0.00	0.00
AGN2	875	2.88	0.81	2.00	0.79	2.01	0.79	0.80
AGN3	875	2.17	0.61	0.00	0.61	0.00	0.00	0.00
AGN4	840	1.99	0.56	0.27	0.56	0.28	0.43	0.44

Notes: N_2 nom = the amount of N_2 in stoichiometric AgN_3; X_{H_2O} nom = mole fraction of H_2O according to the amounts of H_2O and N_2 in the starting material.

heated to 320 °C to decompose AgN_3 (Keppler 1989), and, after about 30 min., heated to the final run temperature. Thermal expansion of the NaCl assemblies raised the pressure to its final run value. Pressure was measured by a strain gauge positioned at the apparatus dead end, and monitored and adjusted automatically by computer in the course of the runs. Although the NaCl assemblies are essentially frictionless (Johannes et al. 1971), and pressure fluctuations during the runs did not exceed a few bars, our determination of the brucite dehydration (Equilibrium 1) in pure H_2O, when compared with the results by Aranovich and Newton (1996, 1997), showed that this type of apparatus requires a pressure correction of about –10% (Table 2). The corrected pressure values are reported hereafter. Due to this correction, the overall pressure uncertainty of our experiments is estimated as ±0.5 kbar.

Detection of reaction

Reaction progress and final fluid composition were detected by a weight-loss method. After quenching an experiment, the unopened Pt capsules were cleaned and re-weighed to check for leakage. A Mettler AE 240 semi-micro-balance with reproducibility of 10^{-5} g was used for weighing. No weight change of the quenched capsules was detected for the successful runs. The capsules were then immersed in liquid N_2 to freeze the water inside, and punctured with a needle while still frozen. An immediate weight loss occurred on warming, indicative of N_2 vaporization. The N_2 yield always coincided, within weighing uncertainty, with that expected from the amount of AgN_3 loaded in the starting material. Two subsequent drying cycles (20 min + 10 min) of a capsule at 150 °C resulted in additional weight loss, attributed to removal of H_2O. In most cases, the weight loss in the second drying cycle was negligible. A water loss greater than the weight of H_2O initially present in the capsule was attributed to brucite decomposition; conversely a drying loss less than the initial H_2O indicated H_2O consumption due to brucite growth. Reaction progress monitored by this technique usually corresponded to about 50–70% reaction in either direction. If the final amount of H_2O determined by the weight-loss technique differed from the initial amount by less than 0.1 mg, the run was considered as "no reaction" and repeated with a starting composition farther off the expected equilibrium value. The direction of reaction progress was confirmed by microscopic inspection of small portions of the charges using an immersion oil with refractive index = 1.548. Brucite was visible as large well-formed rounded or pseudo-hexagonal flakes, almost isotropic due to their planar orientation, but easily distinguishable from periclase by its morphology and low relief, and as rectangular grains with high birefringence, whereas periclase is isotropic and has a high refractive index. Reaction progress was additionally monitored by comparison of the XRD patterns of the recovered charges with those of the standard starting mix. Significant changes in the relative peak heights were observed in all runs, and were always consistent with the results of the other two methods.

RESULTS OF EXPERIMENTS AND DISCUSSION

The experimental brackets of brucite–periclase equilibrium in the presence of H_2O-N_2 fluid are shown in Figure 1. The complete data set is given in Table 3. Most of the complementary half-reversal runs showed reasonably tight convergence on the final fluid composition. The subtle change in curvature

TABLE 2. Results of calibration runs on reaction Br = Per + H_2O in pure H_2O

Run no.	Duration (h)	P_{nom} (kbar)	T(°C)	Stable phase	P_{cor}(kbar)
BPN66	41	15	870	Br	13.3
BPN70	47	15	875	Br	13.3
BPN67	30	15	880	Per	13.3
BPN20	50	10	820	Br	9
BPN25	58	10	825	Per	9
BPN17	40	10	830	Per	9
BPN07-8	24	7	745	Br	5.4
BPN07-9	65	7	750	Br	5.4
BPN07-5	43	7	750	Per	5.4
BPN07-12	24	7	755	Per	5.4

Note: P_{nom} = nominal pressure; P_{cor} = pressure corrected according to the data by Aranovich and Newton (1996) on reaction 1 in pure H_2O (text).

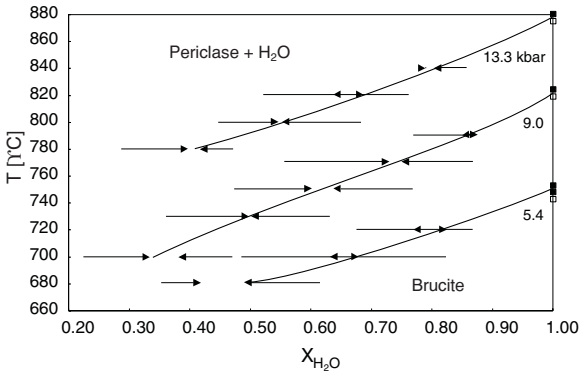

FIGURE 1. Experimental reversals on the reaction Br = Per + H_2O in the presence of the H_2O-N_2 fluids at 5.4, 9 and 13.3 kbar (Table 3). Opposing arrows show fluid composition equilibrated with Br and Per (arrowheads) starting from initial fluids indicated by the arrow tails. Isobaric curves are plotted according to the calculated compositions (Table 4). At X_{H_2O} = 1.0, solid squares show periclase stable, open squares show brucite stable for calibration runs in pure H_2O (Table 2).

TABLE 3. Experimental data on the reaction Br = Per + H_2O in the presence of H_2O-N_2 fluid

Run no.	P (kbar)	T (°C)	Duration (h)	X_{H_2O} start	X_{H_2O} finish	Phase grown
BPN71	13.3	840	49	0.90	0.81	Br
BPN72	13.3	840	49	0.80	0.83	Per
BPN79	13.3	820	25	0.79	0.65	Br
BPN80	13.3	820	25	0.52	0.70	Per
BPN75	13.3	800	45	0.70	0.56	Br
BPN76	13.3	800	49	0.44	0.55	Per
BPN95	13.3	780	64	0.47	0.41	Br
BPN82	13.3	780	60	0.27	0.39	Per
BPN99	9.0	790	47	0.90	0.88	Br
BPN100	9.0	790	47	0.79	0.91	Per
BPN120	9.0	770	39	0.90	0.77	Br
BPN92	9.0	770	60	0.56	0.75	Per
BPN125	9.0	750	95	0.79	0.65	Br
BPN118	9.0	750	49	0.47	0.61	Per
BPN108	9.0	730	90	0.35	0.50	Per
BPN93	9.0	730	47	0.64	0.50	Br
BPN130	9.0	700	37	0.20	0.32	Per
BPN103	9.0	700	69	0.47	0.37	Br
BPN07-16	5.4	720	77	0.69	0.85	Per
BPN07-15	5.4	720	48	0.90	0.79	Br
BPN07-10	5.4	700	42	0.85	0.64	Br
BPN07-11	5.4	700	42	0.48	0.69	Per
BPN07-17	5.4	680	39	0.63	0.49	Br
BPN07-18	5.4	680	39	0.34	0.41	Per

TABLE 4. Midpoints of the experimental brackets and H_2O activity values used in the processing

T (°C)	P (kbar)	X_{H_2O},exp	$\sigma(X_{H_2O})$	a_{HP}	a_{BA}	X_{H_2O}, calc
840	13.3	0.81	0.012	0.852	0.837	0.805
820	13.3	0.68	0.018	0.783	0.767	0.675
800	13.3	0.54	0.017	0.718	0.701	0.557
780	13.3	0.41	0.023	0.655	0.638	0.425
790	9.0	0.87	0.017	0.877	0.876	0.857
770	9.0	0.75	0.014	0.798	0.795	0.738
750	9.0	0.63	0.025	0.723	0.719	0.617
730	9.0	0.5	0.019	0.652	0.647	0.500
700	9.0	0.36	0.024	0.554	0.546	0.368
720	5.4	0.82	0.018	0.850	0.857	0.819
700	5.4	0.67	0.014	0.755	0.761	0.674
680	5.4	0.46	0.018	0.675	0.680	0.503

Notes: Values for H_2O activities calculated for the brucite-periclase equilibrium with two thermodynamic data sets (text): HP = Holland and Powell (1998); BA = Berman and Aranovich (1996); X_{H_2O}, calc = X_{H_2O} calculated with a_{HP} and best fit parameters (Eq. 8) of Equation 6a (text).

of the isobarically univariant lines separating Per and Br stability fields (Fig. 1) is indicative of changes in the mixing properties of fluid species with pressure.

Potential pitfalls associated with the experimental approach of this work would be possible speciation in the H-O-N system that might cause the fluid composition to depart significantly from the true binary, and effect of MgO solubility on the water activity.

To assess the effect of speciation, we assume that the formation of ammonia is the most probable cause of any deviation from binary speciation. The fluid speciation is then governed by reactions:

$$H_2O = H_2 + 1/2O_2 \quad (3)$$

$$3H_2 + N_2 = 2NH_3. \quad (4)$$

At any given T, P, f_{O_2}, and bulk composition $X_{N_2} = 1 - X_{H_2O}$, assuming the molar species fraction of oxygen is negligible, the equilibrium fractions of the remaining species, x_i, where i indexes H_2O (1), H_2 (2), N_2 (3), and NH_3 (4), can be found by solving the following equations derived from thermodynamic (the equilibrium constant) and mass-balance constraints:

$$K_3 = \frac{x_2\gamma_2 f_2^0 \sqrt{f_{O_2}}}{x_1\gamma_1 f_1^0}$$

$$K_4 = \frac{\left(x_4\gamma_4 f_4^0\right)^2}{\left(x_2\gamma_2 f_2^0\right)^3 x_3\gamma_3 f_3^0}$$

$$x_1 + x_2 + x_3 + x_4 = 1$$

$$X_{N2} = x_3 + x_4/2$$

where K_3 and K_4 are the equilibrium constants for Equations 3 and 4, f_i^0 is the fugacity of pure species, and γ_i is its activity coefficient. These equations were solved for a range of f_{O_2} values at 13.5 kbar, 700 °C and $X_{N_2} = 0.7$ and 0.3 using values for the equilibrium constants from Robie and Hemingway (1995), and the fugacities of the pure fluid species and their activity coefficients from Churakov and Gottschalk (2002a, 2002b). The results (Fig. 2) confirm that even at high pressure H_2 and NH_3 are only important species in this system at very low f_{O_2} (compare with Holloway and Reese 1974 at low pressure) and can be neglected for present purposes.

Solubility of MgO is very low in pure H_2O and H_2O-NaCl solutions (e.g., Aranovich and Newton 1997; Newton and Manning 2000a), and in all likelihood should be lower still in the H_2O-N_2 fluids (compare with the effect of CO_2 on the silica solubility: Newton and Manning 2000b; Shmulovich et al. 2001).

The water activity, calculated for each of the experimental brackets P-T according to Equation 2, is given in Table 4. For these calculations, we adopted $\Delta G^0_{P,T}(1)$ and $f^0_{H_2O}(P,T)$ from the thermodynamic data of Holland and Powell (1998) (a_{HP} in Table 4), which exactly reproduces the experimental brackets on Reaction 1 in pure H_2O as obtained by Aranovich and Newton (1996). Essentially the same activity values for the two lower pressures of our experiments are calculated with the thermodynamic data for Reaction 1 from Berman and Aranovich (1996) (a_{BA} in Table 4). For the 13.3 kbar experiments, a_{HP} and a_{BA} values are somewhat farther apart. The discrepancy is caused by the differences in $f^0_{H_2O}(P,T)$ employed in the two data sets. As discussed by Brodholt and Wood (1994) and Aranovich and Newton (1999), the Haar et al. (1984) EOS for H_2O, used by Berman and Aranovich (1996), predicts too low fugacities at pressure above 10 kbar. We therefore based our analysis of the experimental activity–composition relations on the a_{HP} values.

Activity–composition data retrieved from the experiments are shown in Figure 3. There are several sources of uncertainty in these water activities. The uncertainties due to the values for the Gibbs free energy of Reaction 1 are relatively small: ±174 J for the $\Delta G^0_{P,T}(1)$ (Aranovich and Newton 1996; Holland and Powell 1998) and ±100 J for the $f^0_{H_2O}(P,T)$, which translates into a 1–2 relative percentage uncertainty in each of the calculated activities. Experimental P-T uncertainties contribute another 8–10 relative percent. By far the largest uncertainty in the activity–composition relations is that related to the width

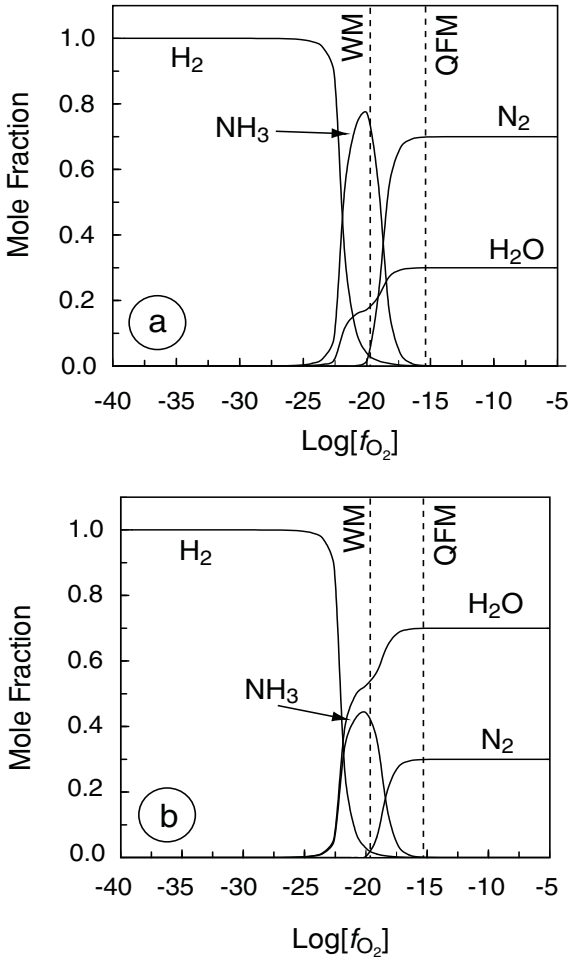

FIGURE 2. Speciation in the system H-O-N as a function of oxygen fugacity at 700 °C, 13.5 kbar, and bulk composition $X_{N_2} = 0.3$ (**a**) and 0.7 (**b**). Fugacities of the fluid species according to the EOS of Churakov and Gottschalk (2002a, 2002b) were employed in the calculations. Oxygen fugacity at the wustite-magnetite (WM) and fayalite-magnetite-quartz (QFM) buffers calculated with the Berman and Aranovich (1996) thermodynamic data set is shown for reference.

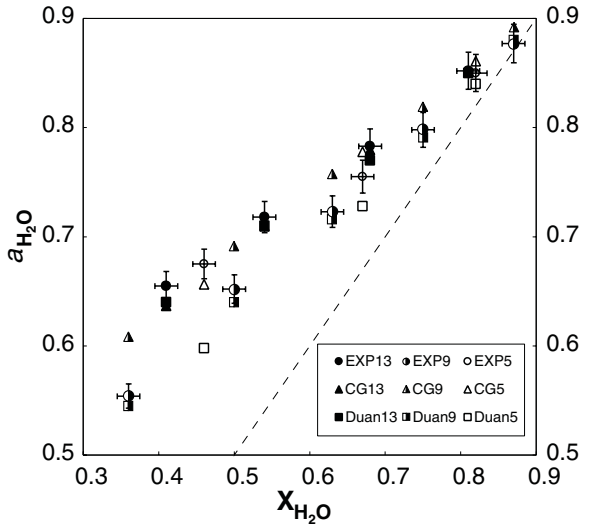

FIGURE 3. Water activity as a function of X_{H_2O} calculated from the brucite-periclase data of Fig. 1 (EXP, circles with uncertainty bars) as compared with the predictions by the EOS of Duan et al. (1996, 2000) (Duan, squares) and Churakov and Gottschalk (2002b) (CG, triangles). Symbols: filled = 13.3 kbar; half-filled = 9 kbar; empty = 5.4 kbar. Ideal mixing line (dashed) shown for reference.

of the compositional brackets on Reaction 1 at each experimental T and P. Both the uncertainties of the weight-loss method and lack of complete equilibration of the run products cause this uncertainty. The weighing uncertainties, taken as two times precision of the balance, are relatively minor for the water-rich runs (±0.003–0.005 in terms of the water mole fraction), but can amount to $\sigma(X_{H_2O}) = \pm 0.01$ for the runs at the lowest temperature/lowest X_{H_2O} at each given P. The half-width of the compositional brackets on reaction 1 does not exceed 0.015 for most runs listed in Table 3. The overall compositional uncertainty of the experiments at each given P and T is a sum of the width of the half-bracket and weighing uncertainty, and is given in Table 4.

Our results show that H_2O–N_2 fluids are characterized by large positive departure from ideal mixing (Fig. 3). This conclusion agrees qualitatively with the previous experimental phase-equilibrium studies at lower pressure and temperature (Chou 1990; Anovitz et al. 1998), as well as with the large positive volume (Basaev et al. 1974) and enthalpy (e.g., Lancaster and Wormald 1990) of mixing. No quantitative comparison can be made because of the lack of direct experimental data in the P-T range of our experiments.

Recently, Duan et al. (1996, 2000) published an EOS that predicts thermodynamic properties of fluids in the system H_2O-CO_2-CH_4-N_2 up to 2000 K and 100 kbar. The EOS of Duan et al. (1996) is based on a combination of the theoretical virial-type equation describing pure fluids with a semi-empirical mixing rule for the fluid mixtures. The mixing model involves two empirical parameters for each binary system to be fit from experimental data on the binaries. Water activity calculated with their equation for the T-P-X_{H_2O} conditions of our experiments agrees well with the experimental values (Fig. 3) but appears to underestimate the degree of non-ideality in this system. Also shown for comparison in Figure 3 are the a_{H_2O} values calculated with the EOS of Churakov and Gottschalk (2002b). These authors derived a model for fluid mixtures based entirely on the equations for the end-member species, which, therefore, makes it less empirical than that of Duan et al. The model of Churakov and Gottschalk (2002b) agrees very well with the experimental values within their uncertainties.

Aranovich and Newton (1999) used an alternative, entirely empirical approach to describing activity-composition relations in binary fluid mixtures for analytical representation of their experimental measurements in the H_2O-CO_2 system. This approach is based on the van Laar equation for the integral excess Gibbs free energy of binary mixtures (e.g., Saxena and Fei 1988):

$$G^{ex} = X_1X_2W\{V_1^0V_2^0/[(V_1^0 + V_2^0)(X_1V_1^0 + X_2V_2^0)]\} \quad (5)$$

where V_1^0 and V_2^0 are the pure end-member volumes, X_1 and X_2 the mole fractions of the components, and W is a regular solution energy parameter as defined by Guggenheim (1952). From Equation 5, the activity coefficients of the solution end-members can be shown to be:

$$RT \ln\gamma_1 = (X_2)^2 W\{V_1^0(V_2^0)^2/[(V_1^0 + V_2^0)(X_1V_1^0 + X_2V_2^0)^2]\} \quad (6a)$$
$$RT \ln\gamma_2 = (X_1)^2 W\{V_2^0(V_1^0)^2/[(V_1^0 + V_2^0)(X_1V_1^0 + X_2V_2^0)^2]\}. \quad (6b)$$

In principle, the W term for various binary fluids can be calculated from intermolecular potentials describing the pair interactions between various types of molecules present in a mixture (Saxena and Fei 1988; Shi and Saxena 1992). Alternatively, W can be treated as an empirical parameter to be calculated by fitting the experimental data into Equations 6a and 6b (Aranovich and Newton 1999). The advantage of Equations 6a and 6b is that they have very simple analytical form and are not linked to any particular EOS for the end-member gases. We used Equation 6a with the W term expanded in T (K) and P (kbar) as

$$W = (A - BT)[1 - \exp(-20P)] + CP^{0.3}T \quad (7)$$

to process the experimental a_{H_2O}–X_{H_2O} data of Table 4. The best-fit parameters, obtained with the standard volumes of H_2O and N_2 from Churakov and Gottschalk (2002a) and the optimization procedure described in Aranovich and Newton (1996), are:

$$A = 40005 \text{ J}, B = 51.735 \text{ J/K}, C = 14.848 \text{ J/(K·kbar}^{0.3}\text{)}. \quad (8)$$

The standard deviation of the midpoints of the experimental compositional brackets from the best-fit equation is only 0.016 (1σ); that is, the calculated equilibrium compositions lie well within the uncertainties of our experiments (see Table 4). The three parameters (see Eq. 8) of the empirical binary model are insensitive, within reasonable limits, to the input volumes of the pure fluids, and therefore may be used along with any reasonably accurate EOS of H_2O and N_2

The a_{H_2O} values calculated with the present model at 500 °C and 0.5 kbar satisfy all the experimental constraints by Anovitz et al. (1998), although they are somewhat higher than their preferred values for the low water compositions (Fig. 4a). Extrapolation with Equation 6a also agrees reasonably well with the Chou (1990) experiments at 600 °C and 2 kbar (Fig. 4b).

A noteworthy feature of the H_2O-N_2 system is the existence of a broad miscibility gap at supercritical P-T conditions, experimentally documented by direct observations in diamond anvil cells by Costantino and Rice (1991) and van Hinsburg et al. (1993). We calculated the solvus in this system with Equations 6 and 7 and the parameters given in Equation 8 by solving numerically the equations that define equilibrium between the coexisting phases at each given pressure and temperature, where γ is the activity coefficient:

$$(\gamma X)'_{H_2O} = (\gamma X)''_{H_2O}$$
$$(\gamma X)'_{N_2} = (\gamma X)''_{N_2}.$$

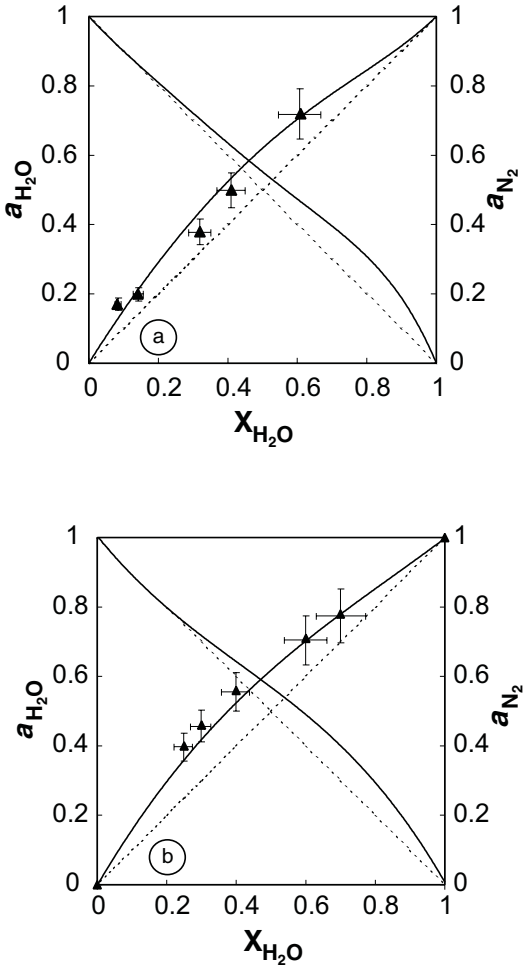

FIGURE 4. Activity–composition relations in the H_2O-N_2 fluids calculated with the present model (curves) as compared with the experimental measurements on the water activity (triangles with uncertainty bars): (**a**) at 500 °C, 0.5 kbar (Anovitz et al. 1998); (**b**) at 600 °C, 2 kbar (Chou 1990).

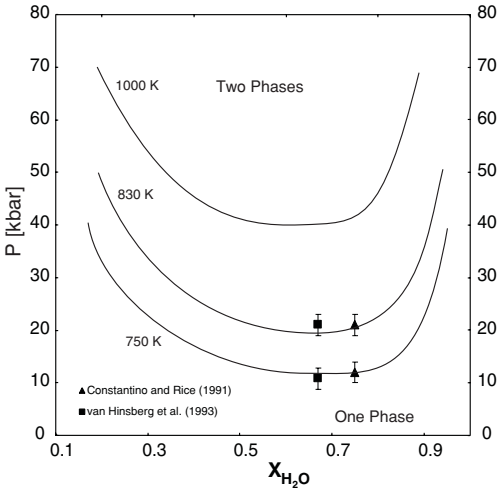

FIGURE 5. Supercritical miscibility gap in the H_2O-N_2 fluid calculated with the present model at three different temperatures (labeled curves) as compared to experimental data by Costantino and Rice (1991) (triangles) and van Hinsberg et al. (1993) (squares).

The results (Fig. 5) are in good agreement with the experimental observations (Costantino and Rice 1991; van Hinsburg et al. 1993) as well as with the predictions of the semi-empirical EOS (Duan et al. 2000, as shown in Fig. 3). Churakov and Gottschalk (2002b) predicted critical pressure (at each given temperature) at the lower limit of the uncertainties of the Costantino and Rice (1991) and van Hinsburg et al. (1993) experiments, which appears to indicate that their model slightly overestimates the activities of the components in this system at very high pressure. The advantage of this model is, however, that it provides accurate activity values without requiring experimental information for fluid mixtures.

ACKNOWLEDGMENTS

This work benefited from much helpful advice by Bob Newton, Larry Anovitz, and Sergei Churakov. Sergei Churakov generously shared the software for calculating fluid species activities prior to its publication. Thanks are due to Zhenhao Duan for calculating the activity values with the EOS of Duan et al. (1996). This work was supported by Swiss National Science Foundation Grant 2100-056980.99/1 and ETH Research Funds Grant 0-20764-00.

REFERENCES CITED

Andersen, T., Burke, E.A.J., and Austerheim, H. (1989) Nitrogen-bearing aqueous fluid inclusions in some eclogites from the Western Gneiss region of the Norwegian caledonides. Contributions to Mineralogy and Petrology, 103, 153–165.

Andersen, T., Burke, E.A.J., and Neumann, E.R. (1995) Nitrogen-rich fluid in the upper mantle: Fluid inclusions in spinel dunite from Lanzarote, Canary Islands. Contributions to Mineralogy and Petrology, 120, 20–28.

Anovitz, L.M., Blencoe, J.G., Joyce, D.B., and Horita, J. (1998) Precise measurement of the activity-composition relations of H_2O-N_2 and H_2O-CO_2 fluids at 500°C, 500 bars. Geochimica et Cosmochimica Acta, 62, 815–829.

Aranovich, L.Y. and Newton, R.C. (1996) H_2O activity in concentrated NaCl solutions at high pressures and temperatures measured by the brucite-periclase equilibrium. Contributions to Mineralogy and Petrology, 125, 200–212.

———(1997) H_2O activity in concentrated KCl and KCl-NaCl solutions at high temperatures and pressures measured by the brucite-periclase equilibrium. Contributions to Mineralogy and Petrology, 127, 261–271.

———(1999) Experimental determination of CO_2-H_2O activity-concentration relations at 600–1000 °C and 6–14 kbar by reversed decarbonation and dehydration reactions. American Mineralogist, 84, 1319–1332.

Basaev, A.R., Scripka, V.G., and Namiot, A.Yu. (1974) The volume properties of mixtures of water vapor with methane and nitrogen at elevated temperatures and pressures. Zhurnal Fizicheskoi Khimii (Russian Journal of Physical Chemistry), 48, 2392.

Berman, R.G. and Aranovich, L.Y. (1996) Optimized standard state and solution properties of minerals: I. Model calibration for olivine, orthopyroxene, cordierite, garnet, and ilmenite in the system FeO-MgO-CaO-Al_2O_3-TiO_2-SiO_2. Contributions to Mineralogy and Petrology, 126, 1–22.

Boyd, S.R., Pineau, F., and Javoy, M. (1994) Modeling the growth of natural diamonds. Chemical Geology, 116, 29–42.

Brodholt, J.P. and Wood, B.J. (1994) Measurements of the PVT properties of water to 25 kbars and 1600°C from synthetic fluid inclusions in corundum. Geochimica et Cosmochimica Acta, 58, 2143–2148.

Chou, I.-M. (1990) Measurement of H_2O activities in N_2-H_2O fluids at 2 kbar and 600°C. Geological Society of America Abstracts with Program, 22, A342.

Churakov, S.V. and Gottschalk, M. (2002a) Perturbation theory based equation of state. I Pure fluids. Geochimica et Cosmochimica Acta, in press.

———(2002b) Perturbation theory based equation of state. II Fluid mixtures. Geochimica et Cosmochimica Acta, in press.

Costantino, M. and Rice, S.F. (1991) Supercritical phase separation in H_2O-N_2 mixtures. Journal of Physical Chemistry, 95, 9034–9036.

De Corte, K., Cartingy, P., Shatsky, V.S., Sobolev, N.V., and Javoy, M. (1998) Evidence of fluid inclusions in metamorphic microdiamonds from the Kokchetav massif, northen Kazakhstan. Geochimica et Cosmochimica Acta, 62, 3765–3773.

Duan, Z., Moeller, N., and Weare, J.H. (1996) A general equation of state for supercritical fluid mixtures and molecular dynamics simulation of mixture P-V-T-X properties. Geochimica et Cosmochimica Acta, 60, 1209–1216.

Duan, Z., Moeller, N., and Weare, J.H. (2000) Accurate prediction of the thermodynamic properties of fluids in the system H_2O-CO_2-CH_4-N_2 up to 2000 K and 100 kbar from a corresponding state/one fluid equation of state. Geochimica et Cosmochimica Acta, 64, 1069–1075.

Franz, G. (1982) The brucite-periclase equilibrium at reduced H_2O activities: some information about the system H_2O-NaCl. American Journal of Science, 282, 1325–1339.

Guggenheim, E.A. (1952) Mixtures. Clarendon Press, Oxford, 365 p.

Haar, L., Gallaher, J.S., and Kell, G.S. (1984) NBS/NRC Steam Tables. Hemisphere Publishing Co., Washington, D.C., 320 pages.

Holland, T.J.B. and Powell, R. (1998) An internally consistent thermodynamic data set for phases of petrological interest. Journal of Metamorphic Geology, 16, 309–343.

Holloway, J.R. and Reese, R.L. (1974) The generation of N_2-CO_2-H_2O fluids for use in hydrothermal experimentation. I. Experimental method and equilibration calculations in the C-O-H-N system. American Mineralogist, 59, 587–597.

Janak, M., Hurai, V., Ludhova L., O'Brien, P.J., and Horn, E.E. (1999) Dehydration melting and devolatilization during exhumation of high-grade metapelites: the Tatra Mountains, Western Carpathians. Journal of Metamorphic Geology, 17, 379–395.

Johannes, W. (1973) Eine vereinfachte piston-zylinder-apparatur hoher genauigkeit. Neues Jahrbuch für Mineralogie, Monatshefte, 337–351.

Johannes, W., Bell, P.M., Mao, H.K., Boettcher, A.L., Chipman, D.W., Hays, J.F., Newton, R.C., and Seifert, F. (1971) An interlaboratory comparison of piston-cylinder pressure calibration using the albite-breakdown reaction. Contributions to Mineralogy and Petrology, 32, 24–38.

Keppler, H. (1989) A new method for the generation of N_2-containing fluids in high-pressure experiments. European Journal of Mineralogy, 1, 135–137.

Knudsen, T.L. and Lidwin, A. (1996) Magmatic CO_2, brine and nitrogen inclusions in Sveconorwegian enderbitic dehydration veins and a gabbro from the bamble sector, southern Norway. European Journal of Mineralogy, 8, 1041–1063.

Lancaster, N.M. and Wormald, C.J. (1990) Excess molar enthalpies of nine binary steam mixtures: new and corrected values. Journal of the Chemical Engineering Data, 35, 11–16.

Mohapatra, R.K. and Murty, S.V.S. (2000) Search for the mantle nitrogen in the ultramafic xenoliths from San Carlos, Arizona. Chemical Geology, 164, 305–320.

Moine, B., Guillot, C., and Gibert, F. (1994) Controls of the composition of nitrogen-rich fluids originating from reaction with graphite and ammonium-bearing biotite. Geochimica et Cosmochimica Acta, 58, 5503–5523.

Newton, R.C. and Manning, C.E. (2000a) Metasomatic phase relations in the system CaO-MgO-SiO_2-H_2O-NaCl at high temperatures and pressures. International Geology Review, 42, 152–162.

———(2000b) Quartz solubility in H_2O-NaCl and H_2O-CO_2 solutions at deep crust-upper mantle pressures and temperatures: 2–15 kbar and 500–900°C. Geochimica et Cosmochimica Acta, 64, 2993–3005.

Robie, R.A. and Hemingway, B.S. (1995) Thermodynamic Properties of Minerals and Related Substances at 298.15 K and 1 bar (105 Pascals) Pressure and at Higher Temperatures. USGS Bulletin 2131.

Rosenbaum, J.M., and Slagel, M.M. (1995) C-O-H speciation in piston-cylinder experiments. American Mineralogist, 80, 109–114.

Saxena, S.K. and Fei, Y. (1988) Fluid mixtures in the C-O-H system at high pressure and temperature. Geochimica et Cosmochimica Acta, 52, 505–512.

Shi, P. and Saxena, S.K. (1992) Thermodynamic modeling of the C-O-H-S fluid system. American Mineralogist, 77, 1038–1049.

Shiryaev, A.A., van Veen, A., Schut, H., Kruseman, A.C., and Zakharchenko, O.D. (2000) Positron beam investigations of natural cubic and coated diamonds. Radiation Physical Chemistry, 58, 625–632.

Shmulovich, K.I., Shmonov, V.M., and Zharikov, V.A. (1982) The thermodynamics of supercritical fluid systems. In S.K. Saxena, Ed., Advances in Physical Geochemistry, p. 173–190. Springer, Berlin.

Shmulovich, K.I., Graham, C., and Yardley B. (2001) Quartz, albite and diopside solubilities in H_2O-NaCl and H_2O-CO_2 fluids at 0.5–0.9 GPa. Contributions to Mineralogy and Petrology, 141, 95–108.

Turner, G., Burgess, R., and Bannon, M. (1990) Volatile-rich mantle fluids inferred from inclusions in diamonds and mantle xenoliths. Nature, 344, 653–655.

van Hinsberg, M.G.E., Verbrugge, R., and Schouten, J.A. (1993) High temperature-high pressure experiments on H_2O-N_2. Fluid Phase Equilibria, 88, 115–121.

Voncken, J.H.L., Vanroermund, H.L.M., Vandereerden, A.M.J., Jansen, J.B.H., and Erd RC (1993) Holotype buddingtonite—an ammonium feldspar without zeolitic H_2O. American Mineralogist, 78, 204–209.

MANUSCRIPT RECEIVED JULY 31, 2001
MANUSCRIPT ACCEPTED JANUARY 27, 2002
MANUSCRIPT HANDLED BY DAVID R. COLE